DOE/ER/13836-12

MESOPOROUS CATALYSTS, SUPPORTS AND CATALYTIC MEMBRANES BASED ON MCM-41

Final Report

for the period January 15, 2000 - January 14, 2001

Gary L. Haller
Department of Chemical Engineering
Yale University
New Haven, CT 06520 - 8286

July, 2001

Prepared for
THE U.S. DEPARTMENT OF ENERGY
AGREEMENT NO. DE-FG02-88ER13836

NOTICE

DISCLAIMER

I. Abstract, Research Objectives and Report Outline

Our objective has been two fold: to understand the effect of pore size on the chemistry and activity of active sites and to investigate both the pore size and anchoring effect of Me-MCM-41 on Pt clusters (where Me is a metal incorporated into silica based MCM-41). We are not focused on the effect of pore size on transport of reactants and products, but on how the local radius of curvature might effect the properties of a foreign ion embedded in a silica wall that acts as a catalytic site or anchor for the catalytic site. The mesoporous molecular sieves, MCM-41, allows the variation of pore size with constant composition and pore geometry so these new materials allow this scientific question to be addressed for the first time.

For the anchoring effect, we have concentrated on Sn-MCM-41 to prepare Pt/Sn-MCM-41 catalysts, by characterizing these and by testing them with probe reforming reactions (dehydrogenation, isomerization and aromatization).

While this is a final report on activity January 15, 2000 - January 14, 2001, this was a continuation of work initiated in the three year grant period January 15, 1997 -January 14, 2000, so the summary of progress for these three years (previously reported in a renewal proposal signed July 26, 1999) is appended for completeness.

This Final Report will list only publications and reports for the January 15, 2000 - January 14, 2001, period and describe research on the Pt/Sn-MCM-41 catalysts in that period. Additional details are given in the appendix.

II. Published and In-Press Reports

Published Articles

"Gas Phase Methanol Oxidation on V-MCM-41," **Applied Catal.,** 188, 277 (1999). With Sangyun Lim.

"Preparation of Highly Structured V-MVM-41 and Determination of Its Acidic Properties," **Stud. Surf. Sci. and Catal.**, 130, 3053 (2000). With Sangyun Lim.

"Several Factors Affecting Al-MCM-41 Synthesis, **Microporous and Mesoporous Materials,** 43, 171 (2001). With Y. Cesteros.

"Synthesis and Characterization of Pt/MCM-41 Catalysts, **Microporous and Mesoporous Materials**, 44-45, 377 (2001). With N. Yao, C. Pinckney, S. Lim and C. Pak.

"Preparation of Vanadium- and Chromium-substituted KIT-1 Disordered Mesoporous Materials by Direct Incorporation, **Microporous and Mesoporous Materials**, 44-45, 321 (2001). With Chanho Pak.

Articles in Press

"Reversible Coordination Change of Chromium in Cr-MCM-41 and Cr-MCM-48 Studied by X-ray Absorption Near Edge Structure, **Microporous and Mesoporous Materials**, 13th IZC, Montpellier, France, July, 2001. With C. Pak.

"Hydrodechlorination of 1,2,4-trichlorobenzene on Ni/Al-MCM-41 Catalysts," **Microporous and Mesoporous Materials**, 13th IZC, Montpellier, France, July, 2001. With Y. Cesteros, P. Salagre, F. Medina, J.E.Sueiras.

III. Research Progress

Metal-support Interactions in Pt/MCM-41

The general preparation procedure for obtaining a reasonably high dispersion for Pt/MCM-41 has recently been published [1]. Here we will review subsequent work on the effects of pore size and K promotion of Pt/MCM-41 on the activity, selectivity and stability of these catalysts for n-hexane reforming reactions (dehyrogenation, isomerization and aromatization). We will also comment on deactivation and regenerability. However, this is primarily background work to compare the effects of Sn addition to the support, Pt/Sn-MCM-41 catalysts, on the activity, selectivity and stability of the resulting catalysts.

The Pt/MCM-41 samples were initially characterized by physical adsorption of N_2 and XRD. These results are summarized for Pt supported on MCM-41 templated with a C12 alkyl chain length surfactant in Table 1. While the loading of Pt is only 1 wt %, there is a very significant loss in pore volume after reduction to the metal. However, this loss is even more extreme after reaction. While it might be dismissed as a result of pore plugging by coke, the apparent increase in unit cell size and surface area suggests that this is more likely the result of destruction of the MCM-41 structure during reaction. This is somewhat surprising but is probably the result of Pt catalyzed hydrogenolysis of Si-O-Si bonds. In fact, the more modest increase in unit cell dimension and loss in pore volume after reduction (at 350°C) than after reaction for several hours at temperatures above 400 °C are consistent with a slow Pt catalyzed hydrogenolysis of the silica framework.

Because reforming reactions are known to be bifunctional and our previous work on substitution of first row transition metals, e.g., V-MCM-41, indicates that there is always an accompanying effect on acidity [2], we have investigated the magnitude of this effect on Pt/MCM-41 by K^+ impregnation. (The K^+ loading was about 0.8 wt % on catalysts of about 1 wt % Pt.) The initial turnover frequency of a Pt/MCM-41 catalyst dropped from 0.07 (sec^{-1}) to 0.04,

but the effect on selectivity is more dramatic increasing the selectivity to benzene and hexenes at the expense of isomerization and hydrogenoloysis. Another interest in this experiment was a comparison between Pt/K-MCM-41 and Pt/K-L-zeolite, the latter being a well-known selective aromatization catalysts. These two catalysts have a common hexagonal pore structure and Pt loading, but the pores of the MCM-41 are significantly larger. While K^+ addition to Pt/MCM-41 most certainly moves it closer to Pt/K-L-zeolite, in no case did we find a Pt/K-MCM-41 catalyst that was competitive with conventional Pt/K-L-zeolite for aromatization selectivity.

While it is probably expected that if a pore size effect is difficult to see when the catalytic site is on the wall where the radius of curvature differs, it is going to be even more challenging to see it reflected in Pt clusters anchored to that surface. The rates (turnover frequency at 460 °C, per sec) appear to follow the dispersion and is just the inverse order of the selectivity to various C6 olefins, a consequence one surmises of the differing structure sensitivity of the several reactions involved in n-hexane reforming. However, hydrogenolysis which is generally considered the most structure sensitive of all the reactions does not obviously parallel the dispersion. The problem here is that the variation in both Pt loading and dispersion is so great that they mask any possible pore size effects so no conclusion can be drawn except that one must

Table 1: Physical Properties of Pt/MCM-41 after different treatments

Sample	Treatment, After	Unit Cell Å	Pore Size Å	Wall Width Å	Surface Area m^2/g	Pore Volume cm^3/g
MCM-41	Fresh	29.6	18.8	10.8	884	0.63
Pt/MCM-41	Drying	30.0	18.4	11.6	787	0.52
Pt/MCM-41	Reduction	31.9	18.4	13.5	629	0.37
Pt/MCM-41	Reaction	34.5	16.6	17.9	668	0.16

Table 2: Rate and Selectivity

Pt on MCM-41 Prepared with	Pt loading wt %	Pt Dispersion	Initial TOF (per sec) at 460°C	C6 Olefin Selectivity, %	C1 - C5 Selectivity, %
C16 alkyl	1.31	0.45	0.16	10	9
C14 alkyl	1.53	0.70	0.07	30	6
C12 alkyl	1.06	0.62	0.12	20	5

get control of the pore size and other synthesis parameters that effect the loading and/ or dispersion before any conclusions about pore size effects can be evaluated.

Metal-support Interactions in Pt/Sn-MCM-41

By characterizing Pt/Sn-MCM-41 by X-ray absorption one can clear show that 1) that Pt and Sn interact in the precursors, 2) that all of the Sn is more reducible in the catalytic presence of Pt, and 3) that some of the Sn is reduced to the metallic state. Solid state NMR of ^{119}Sn can be used to deduce that the Sn is isolated and in tetrahedral coordination (before addition of Pt). Of course, the rates of n-hexane reforming reactions are lower on Pt/Sn-MCM-41 than on Pt/MCM-41 and after several hours on stream (coke build up), the Pt/Sn-MCM-41 catalysts essentially become selective dehydrogenation catalysts and C6 olefins become the dominant product.

The greatest effect of Sn is reflected in greater dispersion of the Pt and in the inhibition of structure loss in the Sn-MCM-41 support relative to the MCM-41 support. Perhaps both of these can be the result of Pt clusters anchoring to the walls of Sn-MCM-41 at the Sn sites which might increase the Pt dispersion (and the stability against sintering) and also isolate the Pt cluster somewhat removed from Si-O-Si bonds and therefore inhibit the hydrogenolysis of these bonds and the accompanying destruction of the MCM-41 structure.

References

1. N. Yao, C. Pinckney, S. Lim, C. Pak, and G. L. Haller, **Microporous and Mesoporous Materials**, 44-45, 377 (2001).

2. S. Lim and G. L. Haller, **Stud. Surf. Sci. and Catal.**, 130, 3053 (2000).

Appendix

I. ***Summary Progress Report***

Summary progress report for the three year grant period January 15, 1997 -January 14, 2000, previously reported in a renewal proposal signed July 26, 1999.

II. ***Published and In-Press Reports***

In the three year period covered by the previous grant, we have published sixteen papers and there is an additional paper in press, all of which acknowledge DOE support. Also listed below are three theses completed using DOE support during the last grant period. Some of these papers, and one thesis, do not involve mesoporous molecular sieves, but are derived from the previous DOE grants. Apart from the listing below, they will not be further commented on in this progress report.

1. Published articles

"Alloy Formation and Stability in Pd-Cu Bimetallic Catalysts," **J. Phys. Chem.**, 100, 16247 (1996) with M.F. Garcia and J.A. Anderson.

"Surface and Bulk Characterisation of Metallic Phases Present During CO Hydrogenation on Pd-Cu/KL-zeolite," **J. Catal.**, 164, 477 (1996) with J.A. Anderson and M.F. Garcia.

"Effect of Pore Size of Mesoporous Molecular Sieves (MCM-41) on Al Stability and Acidity," **Chem. Eng. J.**, 64, 255, (1996) with X. Feng, J.S. Lee, J.W. Lee, J.Y. Lee and D. Wei.

"An X-Ray Absorption Spectroscopy Determination of the Morphology of Palladium Particles in KL-zeolite," **J. Catal.**, 166, 75 (1997) with P. Menacherry and M.F. Garcia.

"Selective Reduction of NO_x with Propene under Oxidative Conditions: Nature of the Active Sites on Copper Based Catalysts," **J. Am. Chem. Soc.**, 119, 2905 (1997) with C. Márquez, I. Rodriguez, A. Guerrero-Ruiz and M. Fernández-Garcia.

"Evaluation of Pore Structure Parameters of MCM-41 Catalyst Supports and Catalysts by Means of Nitrogen and Argon Adsorption," **J. Phys Chem.**, 101, 3671-3679 (1997) with P.I. Ravikovitch, D. Wei, W.T. Chueh, and A.V. Neimark.

"^{71}Ga NMR Characterization of MFI-type Ga-silicate Synthesized by the Rapid Crystallization Method," **Catal. Lett.**, 46, 5-9, (1997) with T. Takeguchi, K. Kagawa, J.-B. Kim, T. Inui and D. Wei.

"The Effect of Water on the Infrared Spectra of CO Adsorbed on Pt/K L-zeolite," **Catal. Lett.**, 44, 135 (1997) with P.V. Menacherry.

"Synthesis and Characterization of Alkali-free, Ga-substituted MCM-41 and Its performance for n-Hexane Conversion," **J. Catal.**, 175, 1 (1998) with T. Takeguchi, J.-B. Kim, M. Kang, T. Inui, and W.-T. Chueh.

"Density Functional Theory Model for Calculating Pore Size Distributions: Pore Structure of Nanoporous Catalysts," **Advances in Colloid and Interface Sciences,** 76-77, 203 (1998) with P.I. Ravikovitch and A.V. Neimark.

"Adsorption Characterization of Mesoporous Molecular Sieves," **Stud. Surf Sci. Catal.,** 117, 77 (1998), with P. I. Ravikovitch and A. V. Neimark.

"Titanium Containing MCM-41 Molecular Sieves Prepared by Secondary Treatment," **Stud. Surf. Sci. Catal.,** 117, 77 (1998), with Anke Hagen and Di Wei.

"Adsorption Characterization of Nanoporous Materials of M41S Type," in Fundamentals of Adsorption 6, Francis Meunier, ed., pp. 545-550, Elsevier (1998) with P. I. Ravikovitch and A. V. Neimark.

"Catalytic Behavior of Vanadium Substituted Mesoporous Molecular Sieves," **Catal. Today**, 51 501 (1999), [Proceedings of the 2nd International Memorial G. K. Boreskov Conference], with D. Wei and W.-T. Chueh.

"Synthesis and Characterization of Vanadium Substituted Mesoporous Molecular Sieves," **J. Phys. Chem.**, 103, 2113 (1999), with D. Wei, H. Wang, X. Feng, W.-T. Chueh, P. Ravikovitch, M. Lyubovsky, C. Li, and T. Takeguchi.

"Synthesis and Properties of Chromium Containing Mesoporous Molecular Sieves," (Proceeding of TOCAT [Tokyo Advanced Catalytic Technology] meeting, Tokyo, July, 1998), Science and Technology in Catalysis 1998, PP. 239-244, Kodansha Ltd. (1999), with D. Wei, N. Yao.

2. Articles in Press

"Gas Phase Methanol Oxidation on V-MCM-41," **Applied Catal.A: General**, with S. Lim.

3. Theses

"Platinum-Tin Bimetallic Catalysts Supported on L-Zeolite: Synthesis and Characterization," Hui Wang, Ph. D. Thesis, Yale University, 1997.

"Synthesis, Characterization and Catalytic Properties of V-, Ti- and Cr-MCM-41," Di Wei, Ph. D. thesis, Yale University, May, 1998.

"Characterization of Nanoporous Materials by Gas Adsorption and Density Functional Theory," Peter I. Ravikovitch, Ph. D. thesis, Yale University, Dec., 1998.

III. ***Progress Review***

We have investigated pore size effects on gas phase oxidation of methanol and ethanol by molecular oxygen over Ti-MCM-41, V-MCM-41 and Cr-MCM-41 [23]. These gas phase reactions are diagnostic, avoid possible complications of transport control in the liquid phase, and of leaching of the first row transition metal ions from the walls of MCM-41. However, we have in each case also performed one or more liquid phase oxidations using larger oxidants and reactants, e.g., alkylaromatics oxidized by tert-butyl hydroperoxide, in both aqueous and non-aqueous solvents. Among these three catalytic systems, Cr-MCM-41 is the least interesting because Cr is oxidized to Cr(VI) during calcination and the resulting material is unstable with respect to the thermal degradation to Cr_2O_3 [24]. The Ti-MCM-41 was prepared by direct incorporation of Ti into the MCM-41 structure during synthesis and also by a secondary

treatment where Ti was substituted for Al in Al-MCM-41 [25]. Such secondary substitutions have been successful for zeolites [26, 27] but were much less so for MCM-41.

In this report, we will focus on Ti-, and V-MCM-41 catalysts which have been most throughly investigated and are the most potentially useful as oxidation catalysts. Both the Ti-MCM-41 (prepared by direct synthesis) and V-MCM-41 are good catalysts for alcohol oxidation but V-MCM-41 has the higher activity [23] and the added advantage that it can be characterized spectroscopically by ^{51}V solid state NMR as well as infrared, Raman, DR-UV and X-ray absorption. Of course, XRD and physical adsorption are also essential characterization tools for mesoporous molecular sieves. Progress and improvements of the latter are first summarized below because they apply to all of the MCM-41 systems investigated and are always used first to determine the success of the synthesis. That is, we are most interested in catalyts which exhibit the highest degree of order as represented in XRD and N_2 isotherms.

1. Characterization of MCM-41 Materials by Physical Adsorption

Mesoporous molecular sieves, i.e., MCM-41 materials, have sufficiently regular pores that the pore walls diffract X-rays but they are not crystalline materials. Thus X-ray diffraction (XRD) and transmission electron microscopy (TEM) are often used to characterize these materials. However, XRD can only detect that portion which is well ordered and TEM samples such a small fraction of a given material that it may not be representative. While physical adsorption requires interpretation, it does measure a global average of the structure, it can be used to directly measure the pore size and pore size distribution and, in conjunction with XRD, allows the determination of the wall thickness.

A concise review of the current understanding of physical adsorption on MCM-41 and related structures may be found in the new text by Rouquerol, Rouquerol and Sing [28]. Some of these materials present an ideal reversible Type IV isotherm with a sharp step over a narrow range of relative pressure. Such truly reversible Type IV isotherms are rare, but often found on well ordered MCM-41 and have been reproduced in several laboratories. Hysteresis is fairly common, even on what are thought to be reasonably well ordered MCM-41 samples, and the origin of hysteresis is still being debated [29, 30]. However, it is generally agreed that pore size and pore size distributions based on methods that use the Kelvin equation (assuming hemispherical meniscus formation) and correcting for the adsorbed layer thickness provide values that should be regarded as apparent rather than real pore sizes.

In P. Ravikovitch's thesis [31], a non-local density functional theory (NLDFT) model has been developed for predicting adsorption/desorption isotherms in nanopores of different geometries over a wide range of pore sizes, and for calculation of pore size distribution from the experimental adsorption isotherms based on given intermolecular fluid-fluid and fluid-solid

potentials. The NLDFT model has been applied to studies of N_2 and Ar adsorption and hysteresis phenomena in MCM-41 materials.

The NLDFT model has been tested against the experiments on reference MCM-41 materials with pore sizes varying form 32 to 45 Å. It has been demonstrated that the NLDFT model gives consistent results with respect to the pore size distributions and pore wall thicknesses. The pore size distributions calculated from N_2 isotherms at 77 K, and from Ar isotherms at 77 and at 87 K were in good agreement, providing that the desorption branches of the experimental isotherms are employed. It should be noted that the good agreement between the results of Ar and N_2 models has been obtained by using, for Ar at 77K, the saturation pressure of the supercooled liquid rather than the experimentally measured saturation pressure of solid Ar because Ar does not freeze at this temperature in the mesopores [32].

The pore wall thickness of MCM-41 materials calculated from conventional methods of pore size analysis, such as Barrett-Joyner- Halenda, are unrealistically large because these methods underestimate the pore size in the range of 20-40Å. The thickness of pore wall of MCM-41 samples was calculated by subtracting the internal pore size from the spacing between pores obtained from XRD. We find the pore wall thickness to be about 6-8Å and that the wall thickness does not vary with pore size in the range of 20-40Å.

On some samples V-MCM-41, the pore size distributions are bimodel, even when only a single wall spacing is observed in the XRD. This may demonstrate that the analysis of physical adsorption provides a more discriminating measure of the ordered structure than does XRD, but of course, the use of combined characterization techniques is the recommended approach. We have modeled the bimodel pore size distribution and show that it could be accommodated by a single cylindrical pore structure with a secondary layered structure although we do not have an explanation for why the apparently ordered layering is not sufficient to diffract X-rays. The bimodel distribution may, in fact, be an artifact of the modelling method and suggests that further work is needed in this field.

2. Synthesis and Characterization of Ti- and V-MCM-41

Conceptionally, the original idea was to seek experimental evidence that the size of a pore, in the lower mesoporous range of about 15Å to 50Å, could affect catalytic activity and/or selectivity. While we were not uninterested in effects that are of transport origin, that was not the primary interest. The chemical question was: Can the local radius of curvature of a pore wall, perhaps reflected in the local bond angles and bond lenghts on a molecular level, change the local chemistry of a catalytic site sufficiently to affect the catalysis on the site? In previous work supported by DOE we had been able to answer this in the affirmative for acid catalyzed reactions where the acid site was created by Al substitution of Si in a MCM-41 structure [20].

Pore size effects for alcohol oxidation on Ti-MCM-41 and V-MCM-41 are quite different from acid catalyzed reactions on Al-MCM-41. The effect is larger in magnitude and activity and pore size have a more complex relationship, i.e., there is an apparent optimum pore size. There are strong parallels between our observations on V-MCM-41 [21, 33] and on Ti-MCM-41 [25, 34]. We will first discuss Ti-MCM-41 because our results on this system are only partially published and then briefly summarize the new work on V-MCM-41.

2.a Ti-MCM-41

The synthesis of Ti-MCM-41 has been carried out under alkali free conditions. A uniform hexagonal pore structure of MCM-41 is reflected in a main peak at $2\theta < 3$ degrees corresponding to the (100) diffraction, accompanied by much weaker (110), (200) and (210) reflections in the 2θ range of 4 to 7 degrees. From the XRD profiles of siliceous MCM-41 and Ti-MCM-41 samples, one intense peak can be seen in the low angle range representing the regular spacing of the pores. The diffraction peaks of (110) and (200) reflections (characteristic of hexagonal pore structure) for selected samples were measured separately. The d_{100} diffraction peak is used as a measure of spacing between the hexagonal layers.

Nitrogen physisorption is another effective tool to obtain information on the pore structure and surface area. A steep capillary condensation without hysteresis is an indication of an uniform mesoporous structure. The pore size distributions for our samples were calculated from the isotherms by using the Non-local Density Functional Theory (NLDFT) model. A detailed description of the theory has been given by Ravikovitch [31]. The pore size distributions indicate a monodisperse structure for Ti-MCM-41 samples.

The presence of a 960 cm^{-1} absorption band in the FTIR spectra of all Ti-containing silicates, and V or Al modified mesoporous materials, may not be taken as proof of incorporation since pure silicates and siliceous MCM-41 also show a similar band. However, a notable increase in the intensity ratio of 960 cm^{-1} band relative to the 800 cm^{-1} band (symmetric stretching vibrations of SiO_4) is observed with the Ti-MCM-41 samples as compared with the siliceous MCM-41 counterpart and this increase may be caused by the incorporation and a measure of it.

In order to study the local environment of Ti-MCM-41 samples, diffuse reflectance UV-visible and X-ray absorption spectroscopy were carried out on samples with different Ti loading and pore size. The Ti-MCM-41 samples exhibit an absorption band at 220 nm which has been assigned to the framework species interacting with water molecules. Moreover, at higher Ti content, the UV absorption band becomes broader and shoulders at 270 nm and 300 nm appear. This suggests that the local environment becomes more distorted and other extra-framework Ti species are formed when the loading is increased. According to Blasco et al. [35] the 270 nm band may be due to the condensed hexacoordinated Ti species. In the case of catalysts with

different pore size, the UV spectra of samples with smaller pores show a band at 210 nm which has been assigned to tetrahedral local symmetry. This indicates that in the smaller pores the Ti sites may not be accessible to water molecules. This phenomena has been observed on V-MCM-41 samples with smaller pore sizes also [33]. In the case of larger pores, the 220 nm band suggests octahedral symmetry resulting from coordination with two water ligands. Furthermore, the results suggest a decreased hydrophobicity with increasing pore size of Ti-MCM-41. The UV edge energy may be correlated with the domain size. The edge position was determined in the classical fashion for allowed transitions by finding the energy intercept of a straight line fitted through the low energy rise in the graphs of $[F(R_\infty) \times h\nu]^2$ vs. $h\nu$, where $F(R_\infty)$ is the Kubelka-Munk function for an infinitely thick sample and $h\nu$ is the energy of the incident photon. The domain size, the so called molecular cage size, could be defined by the nearest neighbor ligands (oxygen in this case) coordinating to the Ti center. In the case of vanadium model compounds and V-MCM-41 samples, the edge energy decreases monotonically with increasing domain size [33]. Here a quite similar phenomena was observed where the edge energy decreases with increasing domain size (from tetrahedral to octahedral symmetry).

The X-ray absorption near edge structure at the Ti K edge contains well defined pre-edge features that are related to the local environment surrounding Ti. It is well known that the pre-edge structure is attributed to 1s-3d transitions, which are dipole-forbidden in free atoms and in environments with inversion centers. For regular octahedral coordination, the pre-edge intensity is expected to be very low, as the structure becomes distorted, the bond angle deviations from 90 degree in octahedra may increase 3d-4p mixing into the final state of the pre-edge transition and increase the absorption cross section. In the case of penta- or tetra-coordinated titanium, the absence of an inversion center creates an intense single peak. A distorted octahedral structure is present in all hydrated samples with different pore size and loading. After dehydration at 300°C, the intensity of pre-edge peak almost doubled, but the theoretical intensity for tetrahedrally coordinated reference compounds is not completely reached. Further heating at 400°C resulted in the intensity approaching that of a regular tetrahedral structure. Consistent with the observation on titanium silicalites [36], this indicates that the octahedral coordination in hydrated samples could take place by either the simple addition of H_2O to Ti centers or as a result of hydrolysis of Ti-O-Si bonds and the formation of TiOH groups, followed by the addition of H_2O to the TiOH groups. By taking off two water molecules, the Ti local structure is transformed from a distorted octahedra to a distorted tetrahedra at lower temperatures. A further loss of a water molecule from the TiOH group and a neighboring silanol group, converts tetrahedral sites with a hydroxyl ligand into regular tetrahedra at higher temperatures since, indeed, dehydroxylation would occur only at higher temperatures.

In order to count active sites of catalysts for methanol or ethanol oxidation, oxygen uptake measurements were performed by using a pulse method after a pretreatment of the samples under approximate reaction conditions (lacking oxidants). The pore wall of MCM-41 is so thin that essentially all titanium are surface sites. Oxygen uptake obtained this way would also allow us to count the actual active sites participating in the oxidation catalysis.

Ethanol oxidation was carried out in the temperature range of 290°C - 330°C. The main product is acetaldehyde with some side products such as $(CH_3CH_2)_2O$, CO, CO_2 and water. The reaction was measured at different contact times by varying the flow rate of the reactants at each temperature. The final reaction rates were obtained after normalization by the active Ti sites which were determined by the oxygen uptake at corresponding temperatures. Finally, the TOF to acetaldehyde at different temperatures is correlated with the pore size of Ti-MCM-41.

A strong effect of pore size on catalytic behavior was observed on this series of Ti-MCM-41 samples. The catalytic activities exhibit a volcano pattern of activities which increase with increasing pore size to a maximum and then decrease. A similar pore size effect has been observed on the V-MCM-41 catalysts also (see below) and was assumed to be related to the change of local bond angles of Si-O-V [21]. While the ring size (of silica units in the wall structure) is varied in these MCM-41 catalysts with the same Ti loading and structure type, the most likely changes that may be induced are the changes of the local Si-O-Ti bond angles. As the T-O-T angle is varied, the fundamental chemical variable is the change in the relative participation of s, p and d orbitals in the bonding. In the case of Si-O-V, this was reflected in the oxidation potential of the V which will quite naturally effect the activity of the V in the catalytic oxidation. Here the observed phenomena gives further evidence of the pore size effect on the oxidation potential and may have similar explanation.

2b. V-MCM-41

Several laboratories have contributed to the recent literature on V-MCM-41 [37, 38, 39] in addition to our own work on this catalyst [21, 33] (also, see references therein). In all studies there is general agreement that the calcined catalyst contains V^{5+} incorporated in the pore wall in a tetrahedral environment (in the dehydrated state). Arnold et al. [37] were primarily interested in the synthesis parameters that affect V content incorporation, a topic we will breifly comment on below, a part of recent unpublished work. Grubert et al. [39] found that direct incorporation by hydrothermal synthesis (as opposed to impregnation or chemical vapor deposition) produced the least amorphous non-porous by-product, but had the smallest fraction of reducible V. They also found that hydrogen reduction was slow relative to re-oxidation by molecular oxygen suggesting that the reduction is the slow step in hydrocarbon oxidation catalysis on V-MCM-41. Chatterjee et al. [38] used a room temperature synthesis, but still found a V^{5+} species in a tetrahedral

arrangement, after calcination, and showed that this species is catalytic for oxidation of toluene and hydroxylation of benzene with H_2O_2 in the liquid phase. None these studies address the pore size effect on catalysis.

We have used the gas phase oxidation of methanol (and ethanol) as a probe reaction. Figure 1 shows the rate of formadehyde production as a function of pore size (varied by the template alkyl chain length used in the synthesis). Note that we have dropped the C12 synthesized V-MCM-41 from this comparison because, while it diffracts X-rays, has a high surface area, and apparently tetrahedral V, the N_2 adsorption isotherm indicates that it is mostly microporous, not mesoporous—and it does not conform to the correlation of the other materials. The effect of pore size on alcohol oxidation catalysis over V-MCM-41 molecular seives exhibits the largest pore size effect we have seen. However, we need to be careful about how we normalize these rates. In Figure 1, we have reduced the catalysts in the reactant (methanol) at the same temperature that was used for the reaction and then titrated the site density by oxygen chemisorption at that same temperature. As long as we keep the temperature of pre-reduction (before oxygen titration), of titration, and of reaction identical, we see the same effect of pore size on catalysis. Based on methanol reduction at 350°C and oxygen titration, it appears that about 0.4 of the incorporated V produces a potential site. This is very much larger than the 14% that Grubert et al. [39] found to be reducible with hydrogen at 500°C. If ethanol is used for reduction instead of methanol, this increases to about 0.8. We do not know if this factor of two is the result of ethanol being a better reductant, or is the result of formation of a methoxide and ethoxide species during reduction which might be expected to react with oxygen in a ratio of a factor of two. When CO is used as the reductant, there is no apparent oxygen uptake and when hydrogen is used as the reductant (also at 350°C) the apparent site density based on oxygen titration exceeds five times the amount of V incorporated, which would imply complete reduction of V^{5+} to metal, but that is most unlikely. It is clear that our synthesis has produced a much more accessible and/or reducible V site than was the case in the work of Grubert et al.

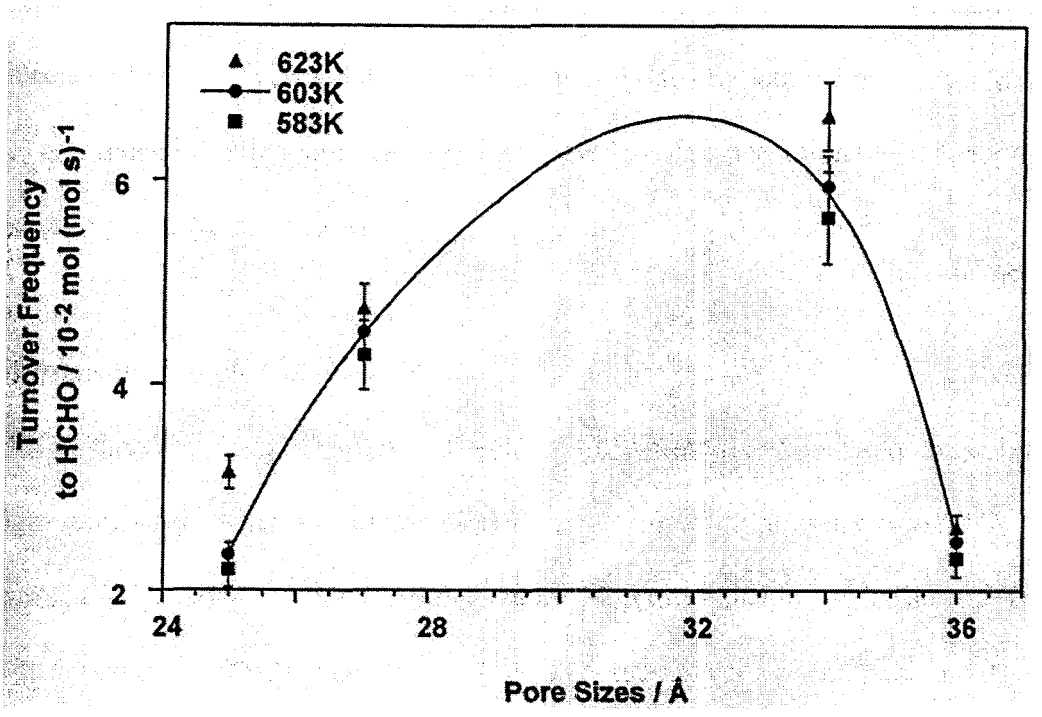

Figure 1. Rate of methanol oxidation with pore size on V-MCM-41.

We have sought to interpret the effect of pore size on alcohol oxidation rates in terms of an effect on the activity of the site. For an oxidation reaction, we assume that some species must be reduced and regenerated by oxidation (reduced first in the case of V^{5+} which is in its highest oxidation state). The Grubert et al. work suggests that the reduction is the slow step and that is consistent with the qualitative reduction (by alcohol) and oxygenation (by molecular oxygen) that we observe in our chemisorption work. It is also generally understood that changes in charge density, molecular orbital configuration, etc., that accompany changes in bond length and bond angle variation will affect the ease of reduction/oxidation. In an attempt to find a direct measure of some electronic property which may be related to redox potential, we have used X-ray absorption near edge structure (XANES).

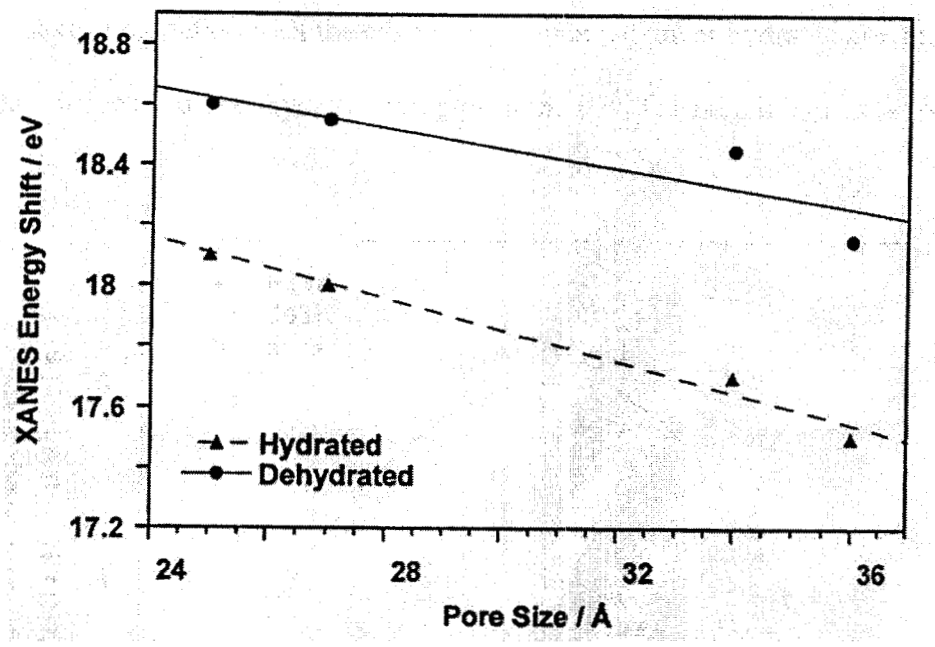

Figure 2. The correlation of V K-edge energies with pore size measured on hydrated and dehydrated V-MCM-41.

The first row transition elements have well-defined site symmetry spectra in the XANES. The relatiave position of the pre-edge peak and K-absorption edge of an element is governed by its chemical state. The energy shift of the edge, the so called chemical shift, is primarily the result of effective charge on the absorbing atom, but its value is also sensistive to the detailed electronic confirguration of the valence band in the absorbing atom. In other words, the energy shift should represent the shift in electron density of the absorbing atom [40], the energy shift is found to follow Kunzl's law and to vary linearly with the valence of the absorbing vanadium atom. The positive shift in the threshold energy corresponds to an apparent increase in valence. More generally, a positive shift of edge energy suggests a decreasing electron density on the atom.

In the present case, the V K-edge energies determined by XANES measurments in the hydrated and dehydrated states are correlated with pore size of V-MCM-41 samples. As shown in Fig. 2, the edge energies decrease linearly with increasing pore size and radius of curvature of the pore wall. A positive shift of edge energy was observed upon dehydration indicating a decreasing electron density on V atoms. This may be attributed to the loss of water molecules from the coordination sphere of the V ion, water being an electron donor. The decreasing electron density with increased pore size apparently makes the V^{5+} site more easily reduced (it is accompanied by a decrease in activation energy of the reaction), but clearly a second effect of pore size sets in and results in a maximun in the rate. One possible negative effect on rate accompanying increasing pore size is a simple decrease in the heat of adsorption of the alcohol,

i.e., a decrease in coverage of the reactant. We will discuss this in more detail and suggest a method of measuring it in proposed future work decribed later. In summary, we have suggested that the rate of V ion reduction increases with pore size (as the radius of curvature increases and bond angles relax), increasing rate, but this is accompanied by a decrease in reactant coverage with pore size, decreasing the rate, and the two opposing effects may account for the observed maximum in rate with pore size.

3. Pt Supported on Sn-MCM-41

Most of the early catalytic work on MCM-41 involved functionization of the silica framework, e.g., Al-MCM-41 [14] for acid catalyzed reactions or Ti-, V- or Cr-MCM-41 of oxidation reactions (see previous section). However, the very high surface area and regular pores also make these MCM-41 materials natural supports for metal catalysis. As supports, one can take advantage of the flexibility of incorporating foreign ions in the silica matrix to form bifunctional catalysts, to use the incorporated ions as anchoring sites for metal clusters and/or promoters to improve selectivity. The first concept, bifunctional reforming activity analogous to Pt supported on acidic alumina, Pt/Al_2O_3-Cl, was the topic of a recent Ph.D. thesis from our laboratory [22]. Junges et al. [41] investigated several metals, preparation routes, and modifications of MCM-41 and, in particular, attributed improved selective hydrogenation of crotonaldehyde to crotylalcohol on Pt/Ti-MCM-41, relatiave to pure siliceous supports, to the SMSI (strong metal-support interaction) effect.

Tin-containing MCM-41 has been synthesized and characterized by Chaudhari et al. [42]. However, their catalytic interest was again in the direct use of Sn-MCM-41 as an oxidation catalyst for the hydroxylation of phenol and 1-naphthol and the epoxidation of norborene. Several analogous Sn containing silica and alumina supported Pt catalyst systems suggest that Pt/Sn-MCM-41 might be a system where Sn could be both an anchor and a promotor for Pt clusters. One analogy is to commercial naphtha reforming catalysts where Pt is supported on a tin-containing alumina support [43]. While these are usually referred to as bimetallic reforming catalysts, commercial catalysts are prepared by supporting Pt on an alumina where the tin has been incorporated by co-precipitation. While not used commerically, silica supports are known to be less interactive with Sn and these have often been studied to emphasize the Pt-Sn interaction/promotion [44]. Yet another analogous system is Pt-Sn/L-zeolite, a system investigated in a DOE supported thesis in our laboratory by Wang [45]. The pore system of L-zeolite is a hexagonal array of parallel channels, just like in MCM-41, but microporous (undulating in diameter between about 7.1 and 12Å), crystalline, and with a Si/Al ratio of three (not ease to duplicate in MCM-41). Supporting Pt on Sn-MCM-41 would appear to combine some attributes from all of these Pt-Sn catalysts. Firstly, substitution of Sn^{4+} for Si^{4+} in the MCM-

41 via direct synthesis of Sn-MCM-41 [42] potentially accomplishes a tin dispersion not accessable using silica gel supports where the Sn is added post precipitation. Secondly, the regular and variable hexagonal pore structure of MCM-41 is a desirable property not available with either normal silica or alumina supports. Thus, ideally Sn-MCM-41 will be a new support for Pt clusters where the Sn sites act as both anchors to disperse and stabilize the small Pt clusters and to interact and promote them.

The synthesis that we and Chaudhari et al. [42] have used are similar, i.e., a hydrothermal synthesis where Sn is added to the synthesis solution as $SnCl_4$ or K_2SnO_3. We have used both Sn sources although the former has the disadvantage of chloride impurities and the latter precludes an alkali free solution. Both studies have used XRD, N_2 physical adsorption, UV-visiable, IR, ^{29}Si and ^{119}Sn solid state NMR to characterize the products. In addition Chaudhari et al. have used Mössbauer spectroscopy (on Sn-MCM-41) and we have used X-ray absorption spectroscopy (on Pt/Sn-MCM-41). There is general agreement between the two studies which indicate that, following synthesis and calcination, Sn^{4+} is mostly in a tetrahedral environment but at higher loading, some octahedral Sn^{4+} is formed. Mössbauer spectroscopy confirmed that a substantial fraction of the Sn can be reduced to Sn^{2+} in a sample with Si/Sn = 83, and while all of the Sn can be re-oxidized to Sn^{4+}, some of it is not restored to the tetrahedral environment.

We have introduced Pt by three methods: incipient wetness impregnation, ion-exchange, and equilibrium adsorption. The challenge is to achieve a high dispersion (hydrogen chemisorption with H/Pt $\approx$ 1), a moderate loading (of order 1 wt%), and retention of the high surface area and hexagonal structure of MCM-41. Equilibrium adsorption of $Pt(acac)_2$ in dicholromethane achieves a 0.5 wt% loading with no loss of structure but the dispersion is low, H/Pt = 0.2. Ion exchange with $Pt(NH_3)_4^{2+}$ in aqueous solution results in a high loading and good dispersion at high pH (9-11), but most of the structure of MCM-41 is destroyed. Ion exchange at low pH (2 - 3) retains the structure of MCM-41, but the loading is very low. A pH of 4 to 5 is a compromise retaining the MCM-41 structure, achieving moderate dispersion (H/Pt = 0.6) and loading (0.3 wt%). X-Ray absorption near edge structure (XANES) indicates that Pt catalyzes the reduction of Sn so that now a portion is reduced to the metal, but both the chemical shift and the whiteline intensity indicates that complete reduction is not achieved. Presumably the un-reduced material is Sn^{2+}, but that is yet to be proven.

Extended X-ray absorption fine structure (EXAFS) analysis of Pt L_3 edge indicates a coordination number of 5.2 for Pt/Sn-MCM-41 compared to 5.6 for Pt/MCM-41. Thus, the dispersion does appear to be improved by the Sn, but likely the apparent dispersion found by H/Pt is an under estimate because hydrogen chemisorption is inhibited by interaction with Sn. That is, from known correlations between EXAFS coordination numbers and hydrogen chemisorption on Pt, a coordination number less than six would imply a H/Pt one or greater [46].

The deduction that follows is that a good dispersion of Pt clusters interacting with Sn has been acheived. Catalytic conversion and selectivity of n-hexane would be consistent with this deduction because the initial rate is high and selectivity to benzene is above 60%, a selectivity approaching Pt/L-zeolite but more than double what one would expect on Pt/SiO_2. The rate and selectivity decrease rapidly in the first two hours, e.g., the benzene selectivity is down to about 40% after two hours. The mechanism of deactivation has not yet been determined. Thus, the investigation of Pt/Sn-MCM-41 and improvements in dispersion, interaction and stability are unfinished business and a part of our continuation proposal.

References

1. J. S. Beck, J. C. Vartuli,W. J. Roth, M. E. Leonowicz, C. T. Kresge, K. D. Schmitt, C. T-W. Chu, D. H. Olson, E. W. Sheppard, S. B. McCullen, J. B. Higgins, J. L. Schlenker., *J. Am. Chem. Soc.* **114**, 10834 (1992).
2. B. C. Gates, *Catalytic Chemistry* (John Wiley & Sons., New York, 1992).
3. W. O. Haag, R. M. Lago, P. B. Weisz, *Faraday Disc. Chem. Soc.* **72**, 317 (1981).
4. M. J. Climent, A. Corma, S. Iborra, M. C. Navarro, J. Primo, *J. Catal.* **161**, 783 (1996).
5. A. W. Adamson, *Physical Chemistry of Surfaces* (John Wiley & Sons, New York, 1990).
6. E. G. Derouane, J.-M. Andre, A. A. Lucas, *J. Catal.* **110**, 58 (1988).
7. S. M. Babitz, B. A. Williams, J. T. Miller, R. Q. Snurr, W. O. Haag, H. H. Kung,*Appl. Catal. A: Gen.* **179**, 71 (1999).
8. J. S. Beck, C. T-W. Chu, I. D. Johnson, C. T. Kresge, M. E. Leonowicz, W. J. Roth, J. C. Vartuli,*US Patent No. 5,108,725* (1992).
9. J. S. Beck, *US Patent No. 5,057,296* (1991).
10. C. T. Kresge, M. E. Leonowicz, W. J. Roth, J. C. Vartuli, *US Patent No. 5,098,684* (1992).
11. C. T. Kresge, M. E. Leonowicz, W. J. Roth, J. C. Vartuli, *US Patent No. 5,102,643* (1992).
12. C. T. Kresge, M. E. Leonowicz, W. J. Roth, J. C. Vartuli, J. S. Beck, *Nature* **359**, 710 (1992).
13. L. Bonneviot, F. Béland, C. Danumah, S. Giasson, S. Kaliaguine, Eds., *Mesoporous Molecular Sieves 1998*, vol. 117 (Elsevieer, Amsterdam, 1998).
14. A. Corma, D. Kumar, *Stud. in Surf. Sci. and Catal.* **117** (1998).
15. R. Ryoo, J. M. Kim, C. H. Ko, *Stud. Surf. Sci. and Catal.* **117**, 151 (1998).
16. T. Tatsumi, K. A. Koyano, Y. Tanaka, S. Nakata, *Stud. Surf. Sci. and Catal.* **117**, 143 (1998).
17. R. A. van Santen, *Theoretical Heterogeneous catalysis* (World Scientific, Singapore, 1991).
18. P. J. O'Malley, J. Dwyer, *J. Phys. Chem.* **92**, 3005 (1988).
19. A. Redondo, P. J. Hay, *J. Phys. Chem.* **97**, 11754 (1993).
20. X. Feng, J. S. Lee, J. W. Lee, J. Y. Lee, D. Wei, *Chem. Eng. J.* **64**, 255 (1996).
21. D. Wei, W.-T. Chueh, G. L. Haller, *Catal. Today* **51**, 501 (1999).
22. W.-T. Chueh, Ph.D. thesis, Yale University (1997).
23. D. Wei, Ph.D. thesis, Yale University (1998).
24. D. Wei, N. Yao, G. L. Haller, *Stud. Surf. Sci. Catal.* **121**, 239 (1999).
25. A. Hagen, D. Wei, G. L. Haller, *Stud. Surf. Sci. and Catal.* **117**, 191 (1998).
26. B. Kraushaar, J. H. C. VanHoof, *Catal. Lett.* **1**, 81 (1988).
27. G. W. Skeels, E. M. Flanigen, *ACS Symp. Series* **389**, 420 (1989).
28. F. Rouquerol, J. Rouquerol, K. Sing, *Adsorption by Powders and Porous Solids: Principles, Methodology and Applications* (Academic Press, London, 1999).
29. W. C. Conner, M. A. Springuel-Huet, J. Fraissard, J. Bonardet, T. McMahon, L. Boudreau, J. Masciadrelli,*Stud. Surf. Sci. Catal.* **117**, 575 (1998).
30. P. I. Ravikovitch, S. C. O'Domhnaill, A. V. Neimark, F. Schüth, K. K. Unger, *Langmuir* **11**, 4765 (1995).

31. P. I. Ravikovitch, Ph.D. thesis, Yale University (1998).
32. P. I. Ravikovitch, G. L. Haller, A. V. Neimark, *Stud. Surf. Sci. Catal.* **117**, 77 (1998).
33. D. Wei, H. Wang, X. Feng, W.-T. Chueh, P. Ravikovitch, M. Lyubovsky, C. Li, T. Takeguchi, G. L. Haller,*J. Phys. Chem.* B**103**, 2113 (1999).
34. D. Wei, A. Hagen, P. Ravikovitch, X. Feng, G. L. Haller, *J. Catal.* (submitted).
35. T. Blasco, A. Corma, M. T. Navarro, J. Pérez-Pariente, *J. Catal.* **156**, 65 (1995).
36. B. Notari, *Adv. Catal.* **41**, 253 (1996).
37. A. B. J. Arnold, J. P. M. Neiderer, T. E. W. Niessen, W. F. Hölderich, *Microporous and Mesoporous Mater.* **28**, 353 (1999).
38. M. Chatterjee, T. Iwasaki, H. Hayashi, Y. Onodera, T. Ebina, T. Nagase,*Chem. Mater.* **11**, 1368 (1999).
39. G. Grubert, J. Rathousky, G. Schulz-Ekloff, M. Wark, A. Zukal, *Microporous Mesoporous Mater.* **22**, 225 (1998).
40. J. Wong, F. W. Lytle, R. P. Messmer, D. H. Maylotte, *Phys. Rev.* B**30**, 5596 (1984).
41. U. Junges, S. Disser, G. Schmid, F. Schüth, *Stud. Surf. Sci. Catal.* **117**, 391 (1998).
42. K. Chaudhari, T. K. Das, P. R. Rajmohana, K. Lazar, S. Sivasanker, A. J. Chandwadkar,*J. Catal.* **183**, 281 (1999).
43. J. M. Parera, N. S. Figoli, in *Catalytic Naphtha Reforming: Science and Technology* G. J. Antos, A. M. Aitani, J. M. Parera, Eds. (Marcel Dekker, Inc., 1995).
44. G. Meitzner, G. H. Via, F. W. Lytle, S. C. Fung, J. H. Sinfelt, *J. Phys. Chem.* **92**, 2925 (1988).
45. W. Wang, Ph.D. thesis, Yale University (1997).
46. B. J. Kip, R. B. M. Duivenvoorder, D. C. Koningsberger, R. Prins, *J. Catal.* **105**, 26 (1987).
47. S.-J. Jong, J.-F. Wu, A. R. Pradhan, H.-P. Lin, C.-Y. M. a. S.-B. Liu, *Stud. Surf. Sci. Catal.* **117**, 543 (1998).
48. S. Savitz, F. Siperstein, R. J. Gorte, A. L. Myers, *J. Phys. Chem.* B**102**, 6865 (1998).
49. W. O. Haag, R. M. Dessau, in *8th Intern. Cong. on Catal.* . (Verlag Chemie, Berlin, 1984), vol. II, pp. 305.
50. W. O. Haag, R. M. Dessau, R. M. Lago, *Stud. Surf. Sci. Catal.* **60**, 255 (1991).
51. T. F. Narbeshuber, H. Vinek, J. A. Lercher, *J. Catal.* **157**, 388 (1995).
52. A. Corma, V. Fornés, M. T. Navarro, J. Pérez-Pariente, *J. Catal.* **148**, 569 (1994).
53. T. Takeguchi, J.-B. Kim, M. Kang, T. Inui, W.-T. Chueh, G. L. Haller, *J. Catal.* **175**, 1 (1998).
54. S. Lim, G. L. Haller, *Appl. Catal. A: General* , in press (1999).
55. G. Larsen, G. L. Haller, *Catal. Today* **15**, 431 (1992).
56. G. Saracco, V. Specchia, *Catl. Rev.—Sci. Eng.* **36**, 305 (1994).
57. J. E. Martin, M. T. Anderson, J. Odinek, P. Newcomer, *Langmuir* **13**, 4133 (1997).
58. M. Ogawa, H. Ishikawa, T. Kikuchi, *J. Mater. Chem.* **8**, 1783 (1998).
59. R. Ryoo, C. H. Ko, S. J. Cho, J. M. Kim, *J. Phys. Chem. B* **101**, 10610 (1997).
60. H. Yang, N. Coombs, I. Sokolov, G. A. Ozin, *J. Mater. Chem.* **7**, 1285 (1997).
61. H. W. Hillhouse, T. Okubo, J. W. v. Egmond, M. Tsapatsis, *Chem. Mater.* **9**, 1505 (1997).
62. P. Chou, M. A. Vannice, *J. Catal.* **107**, 129 (1987).
63. S. D. Lin, M. A. Vannice, *J. Catal.* **143**, 539 (1993).